Change Detection in Multi-Temporal TerraSAR-X SAR Images Using a Hierarchical Markov Model on Regions

Jie Liu[1], Wen Yang[1,2], Gui-Song Xia[2], Mingsheng Liao[2]
[1] School of Electronic Information, Wuhan University, Wuhan, 430072, China
[2] Key State Laboratory LIESMARS, Wuhan University, Wuhan, 430072, China

ABSTRACT

This paper addresses the problem of change detection in high-resolution multi-temporal synthetic aperture radar (SAR) images (e.g. TerraSAR-X SAR images). Given two images, the proposed method first computes a difference map between them, by taking into account both the spatial and temporal correlations. Change detection is then formulated as a binary (changed/unchanged) segmentation problem of the difference map. A hierarchical Markov model (HMM) is defined on the multi-scale oversegmented regions of the difference map. The change map is finally inferred by relying on the hierarchical marginal posterior mode (HMPM) of the HMM. Experimental results on multi-temporal TerraSAR-X SAR images demonstrate the effectiveness and the reliability of the proposed approach.

Index Terms—Synthetic aperture radar (SAR), change detection, region adjacency graph (RAG), hierarchical Markov model (HMM).

1. INTRODUCTION

Detecting and analyzing temporal changes of land covers at different times is one of the main applications of satellite-based remote sensing. With multi-temporal synthetic aperture radar (SAR) imagery at two given dates, it is possible to identify where changes have taken place and which types of change transitions have occurred. For instance, change detection techniques have been developed for the temporal tracking of multiyear sea-ice floes, flood mapping and urban spatial planning [1]. In recent years, change detection in high-resolution (SAR) images (e.g. TerraSAR-X SAR images) has attracted much attention. However, the diversity of land-covers and the lack of ground truth make the task very challenging.

Depending on the availability of prior information, one could classify the change detection methods for SAR images into two categories: supervised approaches and unsupervised ones. This paper focuses on an unsupervised change detection technique, *i.e.*, to automatically discriminate all the change transitions occurred in an investigated region. Specifically, we use a region-based change detection scheme, by relying on a hierarchical Markov model (HMM) defined on a multi-scale region adjacency graph (RAG) of images [2]. The proposed method has three highlights.

(1) First, to derive a difference map (DM) between two SAR images, we use Kullback-Leibler (KL) distance [3] to calculate their similarity.

(2) Secondly, an edge-aware linear scale space within the framework of local Laplacian filters [4] is used to represent images. We perform a gradient watershed transformation on the scale space to detect a set of over-segmented regions at each scale. A multi-scale region adjacency graph (MRAG) is then built by linking adjacent regions on the scale space.

(3) Thirdly, the hierarchical marginal posterior mode (HMPM) [5] is used to infer the HMM on the MRAG.

By exploiting structures in a hierarchical way, the resulted method is capable of identifying the change transitions at different scales.

In the remainder of this paper, Section 2 details the change detection scheme: computing the difference map, the construction of the MRAG and the HMPM inference. Section 3 shows the experimental results and analyzes the performance. Section 4 concludes and presents perspectives.

2. METHODOLOGY

The proposed change detection framework is illustrated in Figure 1. Like most of change detection methods, a preprocessing step is used for geometric calibration and de-speckling. The change detection scheme then consists of three main steps: computing the scale space of regions, constructing the MRAG and HMPM inference.

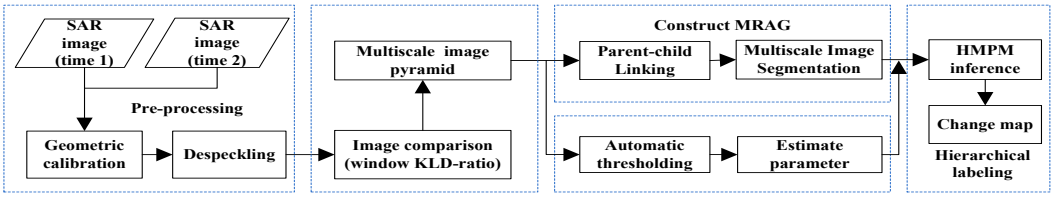

Fig.1 The flow chart of change detection

A. Computing the difference map (DM)

Let X_1 and X_2 be two registered SAR intensity images, acquired over the same geographical areas but at different times t_1 and t_2 ($t_1<t_2$), respectively. To avoid the influence of coherent stained noise as much as possible, we propose to use *KL* distance [4] to obtain a DM image between X_1 and X_2, with the assumption of log-normal distribution of data. More precisely, denoting $f_X(x)$ and $f_Y(y)$ as the probability distribution function (PDF) of the variables X and Y, the *KL* divergence is defined as:

$$K(Y \mid X) = \int \log \frac{f_x(x)}{f_y(x)} f_x(x)dx. \qquad (1)$$

In this paper, we assume that intensity distribution of the images can be well approximated by log-normal distribution. And in order to solve the asymmetry of *KL* distance, we use the following expression instead of *KLD* in (1),

$$\gamma_{KLD} = \int \log \frac{f(x)}{f(y)} f(x)dx + \int \log \frac{f(y)}{f(x)} f(y)dy$$
$$= \frac{1}{2}\left(\frac{\sigma_1^2}{\sigma_2^2} + \frac{\sigma_2^2}{\sigma_1^2}\right) + \frac{1}{2}(\mu_1 - \mu_2)^2 \left(\frac{1}{\sigma_1^2} + \frac{1}{\sigma_2^2}\right) - 1 \qquad (2)$$

where and are the mean and standard variations of M × M patch around central pixel.

A difference map between the images X_1 and X_2 can be computed by comparing patches around the central pixel at corresponding locations, relying on KL distance.

Starting from the difference map, change detection is formulated as a binary (changes/un-changes) segmentation problem. In the following part, we first introduce a multi-scale representation of the DM image.

B. Multi-scale image over-segmentation

This subsection describes how to compute the multi-scale image over-segmented regions. We use a Laplacian pyramid to represent an image. More precisely, for a given image, the original one is considered as the highest resolution, and lower resolutions are obtained by smoothing the original image successively with local Laplacian filters [4]. It allows us to change the coefficient of smoothing filters to produce a series of low-resolution images, and meanwhile guarantee the stability of the boundary between the adjacent regions.

At each scale on the pyramid, the image is partitioned into a number of regions. For its simplicity and efficiency to execute, we use watershed segmentation method to partition an image. Notice that, the ridge tops in gradient magnitude of the images usually mark the edges of objects. In fact, the gradient magnitude is often used to guide the watershed lines to follow the crest lines. Thus, in this paper, we utilize gradient-based watershed transformation to detect a set of regions with well-localized contours.

Observe that, as the coefficient of the smoothing filter changes, the edges separating homogeneous regions are gradually removed, and the intensity minima associated with these regions is annihilated. Then, intensity minima surrounded by taller and wider image edges persist longer in scale-space. Finally, the regions at the finest scale are tracked across the scales [6], using the duality between the regional minima of the gradient and the catchment basins of the watershed. As a result, an image at each considered scale is partitioned into disjoint regions.

C. Construction of the MRAG

The aim of this subsection is to construct the MRAG, by linking the multi-scale regions. The proposed linking process relies on the concept of the dynamics of contours in the scale-space. It is important to observe that, at a segmented scale, each gradient minimum falls into only one region and each region only contains one minimum. Based on this property, a one-to-one mapping is attributed between the regional minima and the catchment basin. This is achieved by projecting a regional minimum at each scale in a coarse one, in other words, if a regional minimum falls in the catchment basin of a regional minimum in coarser scale, then the minimum residing in a given scale is linked with a region in a coarser scale. Following this procedure, the MRAG which depicts the relationship of a child region and a parent region are constituted.

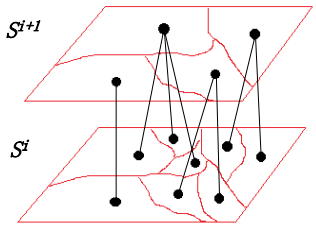

Fig.2 The child-parent relationship on the MRAG

Figure 2 illustrates the MRAG that represents the hierarchical relationship of two-scale over-segmented regions of an image. Let S^i denote the over-segmented regions at a considered scale, and S^{i+1} indicates the corresponding over-segmented region at a coarser scale. If the region gradient minima at S^i are spatially projected on S^{i+1}, then an edge is added to the tree to link these two regions at different scales. If each region is regarded as a node on the tree, the node in S^{i+1} is a parent node, and the node in S_i is a child node. Apart from the coarsest scale, a node in each level has only one predecessor (parent node) in the MRAG. To simplify the expressing, we think that s^- stands for the parent of a node s, while s_- denotes the child of s, and $d(s)$ represents all descendants of s, including s.

D. HMPM inference

The remainder problem is to assign a label (changed/un-changed) to the node of the MRAG. Compared to the

traditional MRF modeling, HMPM estimation is more suited on computational complexity. Additionally, in most cases hierarchical structure can produce considerable effective results due to its capacity to capture the intrinsic multi-scale nature of objects in an image. Ina non-iterative way, modes of posterior marginal (MPM) inference is performed exactly, by propagating information first from the leaves to the root, and then in the reverse direction. In this subsection, we describe the HMPM inference approach.

Let G=(S, L) be a graph composed of a set of nodes *S* and a set of edges *L*. A tree is a connected graph with no cycles, where each node apart from the root *r* has a unique predecessor on the path to the root. The set of nodes *S* can be partitioned into scales, $S = S^0 \cup S^1 \cdots S^N$, according to the path length of each node to the root. S^N stands for the coarsest scale, and S^0 is the leaves formed by segmenting the original image.

We consider a labeling process which assigns a class label x_s to each node of *G*, where x_s takes its values in the set $C = \{\omega_c, \omega_u\}$, of the change or un-change. A number of conditional independence properties are assumed here.

$$p(x^n \mid x^k, k > n) = p(x^n \mid x^{n+1}). \tag{3}$$

To simplify notation, we denote the discrete probability $p(X=x)$ as $p(x)$. It is also assumed that the probabilities of inter-scale transitions can be factorized in the following way [5]:

$$p(x^n \mid x^{n+1}) = \prod_{s \in S_n} p(x_S \mid x_{S^-}). \tag{4}$$

This means that, for each S^n, the conditioning in S^{n-1} reduces to the dependence from its parent node only. Finally, for the observation field, the conditional distribution of the observation Y is expressed as following product.

$$p(y \mid x^n) = \prod_{s \in S^n} p(y^n \mid x^n). \tag{5}$$

To derive the conditional likelihoods $p(y_s|x_s)$, a Gaussian model was chosen, defined by the parameter vector $\theta_i^n = (\mu_i^n, \delta_i^n)$, where μ_i^n is the mean and δ_i^n is the standard deviation of class *i* at the *n*-th level. For the transition probability, we adopted the Potts-like distribution as used by Bouman [7]. This model favors identity between the parent and children, all other transitions being equally likely.

$$p(x_S \mid x_{S^-}) = \begin{cases} \alpha_n & if \quad x_S = x_{S^-} \\ \dfrac{1-\alpha_n}{M-1} & otherwise. \end{cases} \tag{6}$$

Herein, the α_n parameter is the probability that the labeling will remain the same from scale n+1 to n, and it can be estimated using Expectation Maximization (EM) algorithm as discussed in [7]. A. Katartzis[5] describes the hierarchical bottom-up analysis and top-down analysis in details.

3. EXPERIMENTD AND DISCUSSIONS

In this section, we provide the reader with some practical indications and describe experiment setting in this letter. Additionally, the recently developed approaches given in [5] (HMRF-based approach) which are implemented using the same set of parameters as presented in that letter and *FCM* (Fuzzy C means) detailed in [12] are treated as a contrast to our approach.

A. Dataset and experiment setting

In order to assess the effectiveness of the proposed approach, we considered two real data of the downtown (a) in San Francisco and a harbor (b) in Sendai (Japan), see in Figure 3. Two TerraSAR-X images over the downtown of San Francisco respectively acquired on 5th Dec 2007 and 13th Oct 2011 describe the changes including demolition of the building and ships parked near the coast. The second data consisted of two pairs of TerraSAR-X images acquired on Oct 20, 2010 and March 12, 2011, around Sendai, represents changed backscattering coefficients due to a tsunami on March 11, 2011. Both of them have been properly registered to a common spatial geometry of 1m× 1m and two regions of 900×900 pixels has been selected (see Figure 3). In order to facilitate the expression, the previous time will be referred to as t1, whereas the later date will be referred to as t2. To derive the DM image, we choose the 21 × 21 pixels. For the simplicity of computational complexity, three Hierarchical levels are considered in this paper. The hand-labeled ground truth of the change detection map is obtained by two corresponding high resolution optical satellite images as shown in Figure 3.

B. Experimental results and discussions

In our algorithms, detection and inference take place at the regional segments, but the results are propagated to pixel level for visualization and performance evaluation. Change detection results have been evaluated in terms of: percentage overall accuracy *OA%* (*i.e.,* the percentage of samples correctly identified as both changed or unchanged over the whole number of samples), producer's accuracies *Pc%* and *Pu%* of changed and unchanged samples (i.e., the percentage of samples correctly identified as changed/unchanged over the whole number of samples actually changed/unchanged), and *kappa* coefficient of accuracy (which also takes into consideration errors and their types) [8]. In the table 1, we show the comparison of detection accuracies between different methods. And we can clearly see that the capability of our method to capture the details of the changes and the integrity of the regional division seems to be better than other methods. More than that, our method almost reveals all the changed regions in a considerable area with a small amount of interference from Figure 3. However, the regional contours of detection cannot match the ground-truth perfectly. In fact, the boundary of an object in reality always displays the visual

continuity and smoothness of appearance, which means, only the segmented contours endowed with coherence can reflect the real regional border. In response to the point, how to slack the arcs of segmentation properly is a deserving way to make an improvement in the future.

Table 1. Comparison of detection accuracies with HMRF (the same set of parameters as presented paper), FCM-MRF and our method

data	method	OA%	Pc%	Pu%	kappa
a	HMRF	95.33	84.37	95.66	0.7973
	FCM-MRF	96.83	90.53	96.18	0.7681
	Ours	98.40	86.85	97.99	0.8479
b	HMRF	95.45	86.22	97.18	0.8126
	FCM-MRF	97.67	89.62	94.66	0.8034
	Ours	97.62	88.56	96.68	0.8692

4. CONCLUSION

We have presented an efficient and effective change detection approach of high-resolution SAR imagery based on a hierarchical Markov model on the over-segmented regions of the image. The preliminary experimental results show that using multi-scale information can provide satisfied results, which can significantly reduce noise interference, capture the details of the changes and maintain the harmony in regions. In current experiments, we only use the regional linking relationship between the sequential scales and ignore the connection between adjacent regions at a considered scale. In future work, we intend to employ more effective methods for scale generator and take the adjacent correlation at a scale into account during inference.

ACKNOWLEDGEMENT

The research was supported in part by the National Key Basic Research and Development Program of China under Contract 2013CB733404, the Chinese National Natural Sciences Foundation grants (NSFC) 61271401 and research fund of the Key Laboratory of Geo-informatics of National Administration of Surveying, Mapping and Geo-information, No. K201203. The experimental datasets are provided by Digital Globe, Atrium Services, and the United States Geological Survey (USGS) for 2012 IEEE GRSS Data Fusion Contest. We sincerely appreciate them to offer the datasets.

REFERENCES

[1] G. Trianni, E. Angiuli, "Statistical analysis of aniso-tropic rotation-invariant textural measurements of human settlements from multitemporal SAR data," *Joint Urban Remote Sensing Event (JURSE)*, pp.117-120, April 2011.

[2] F. Tupin, M. Roux, "Markov Random Field on Region Adjacency Graph for the Fusion of SAR and Optical Data in Radargrammetric Applications," *IEEE Trans. Geosci. Remote Sens.*, vol.43, no.8, pp.1920-1928, 2005.

[3] S. Kullback, "The Kullback-Leibler distance," *The American Statistician*, vol.41, no.4, pp.340-341, 1987.

[4] S. Paris, S. W. Hasinoff, Kautz, "Local laplacian filters: Edge-aware image processing with a laplacian pyramid," *ACM Trans. Graph*, vol.30, no. 4, pp.1-12, Jul. 2011.

[5] A. Katartzis, I. Vanhamel, H. Sahli, "A hierarchical Markovian model for multiscale region-based classification of vector-valued images," *IEEE Trans. Geosci. Remote Sens.*, vol.43, no.3, pp.548-558, Mar. 2005.

[6] I. Vanhamel, I. Pratikakis, "Multiscale Gradient Watersheds of Color Images," *IEEE Trans. Image Process.*, vol. 12, no. 6, pp.617-626, Jun. 2003

[7] C. A. Bouman, M. Shapiro, "A Multiscale Random Field Model for Bayesian Image Segmentation," *IEEE Trans. Image Process.*, vol. 3, no. 2, pp.162-178, 1994.

[8] D. F. Prieto, M. Marconcini, "A Novel Partially Superv-ised Approach to Targeted Change Detection," *IEEE Trans. Geosci. Remote Sens.*, vol.49, no.12, pp.5016-5038, 2011

[9] F. Luo, W. Yang, Q. Wu, W. Yan, "A Clustering Approach for Change Detection in SAR Images", *9th European Conference on Synthetic Aperture Radar* 2012, 23-26, Nuremberg, Germany, April 2012.

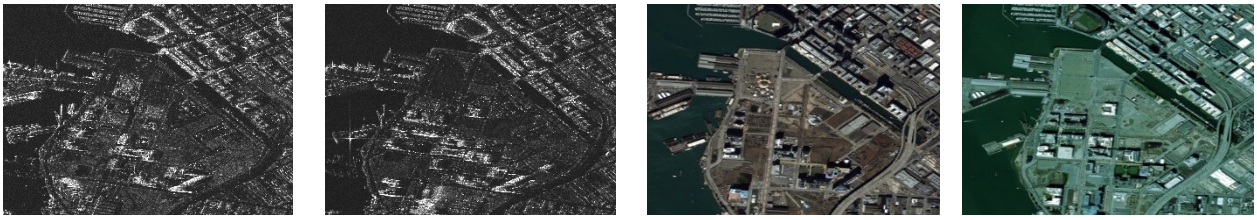

(a) TerraSAR Image(5 Dec. 2007) (b) TerraSAR Image(13 Oct. 2011) (c) Quickbird Image(11 Nov. 2007) (d) WorldView2 Image(9 Oct. 2011)

(e) the hand-labeled ground truth (f) the result of HMRF [5] (g) the result of FCM-MRF [9] (h) the result of our method

Fig. 3 The results of change dectection. (a)-(b) are two TerraSAR-X SAR images of downtown in San Francisco, with size of 2000 × 2000 pixels, and (c)-(d) correspond to the optical images; (e) is the human labeled ground truth; (f)-(g) are the change maps with HMRF, FCM-MRF and our method.